Magnetic circular dichroism at transition metal $L_{2,3}$ edges in $D0_3$-type $(Fe_{1-x}V_x)_3Al$ alloys

Osamu Yoshimoto,[a] Masahiko Kato,[a] Kazuo Soda,[a]* Hiroshi Nozaki,[a] Tsunehiro Takeuchi,[a] Uichiro Mizutani,[a] Masaaki Kato,[b] Yoichi Nishino,[b] Shin Imada,[c] Shigemasa Suga,[c] Tomohiro Matsushita,[d] and Yuji Saitoh[e]

[a]Graduate School of Engineering, Nagoya University, Furo-cho, Chikusa-ku, Nagoya 464-8603 Japan, [b]Department of Materials Science and Engineering, Nagoya Institute of Technology, Gokiso-cho, Showa-ku, Nagoya 466-8555 Japan, [c]Graduate School of Engineering Science, Osaka University, Machikaneyama, Toyonaka 560-8531, [d]Japan Synchrotron Radiation Research Institute, Kouto, Mikazuki-cho, Sayo-gun, Hyogo 679-5198 Japan, [e]Department of Synchrotron Radiation Research, Japan Atomic Energy Research Institute, Kouto, Mikazuki-cho, Sayo-gun, Hyogo 679-5148 Japan.
E-mail : j45880a@nucc.cc.nagoya-u.ac.jp

Magnetic circular dichroism (MCD) spectra have been measured at the Fe and V $L_{2,3}$ edges of $D0_3$-type $(Fe_{1-x}V_x)_3Al$ in order to investigate their local magnetic moments and electronic structures. Large MCD is observed at the Fe $L_{2,3}$ edges, while the V $L_{2,3}$ MCD shows relatively small intensity with complicated features. Signs of these MCD spectra indicate an antiferromagnetic coupling between the magnetic moments on Fe and V. According to the analysis based on the magneto-optical sum rules, the magnetic moment decreases with x, but remains fairly large for Fe_2VAl, which might arise from its marginally magnetic nature.

Keywords : magnetic circular dichroism, local magnetic moments, $D0_3$-type $(Fe_{1-x}V_x)_3Al$ alloys, Fe $L_{2,3}$ edges, V $L_{2,3}$ edges

1. Introduction

In the $D0_3$-type pseudo-binary $(Fe_{1-x}V_x)_3Al$ alloys, the partial substitution of V for Fe in the $D0_3$-orderd ferromagnet Fe_3Al results in an anomalous negative temperature dependence of their electrical resistivily and a remarkable reduction in Curie temperature and average magnetic moment (Nishino *et al*., 1997, Kato *et al*., 2000). In particular, the Heusler-type Fe_2VAl (the alloy $(Fe_{1-x}V_x)_3Al$ with x=1/3) exhibits a semiconductor-like behaviour with a resistivity reaching 30 μΩm at 4 K, the disappearance of the magnetic ordering, and the enhancement of the effective electron mass at low temperatures. These physical properties have strong similarities to those observed in the heavy fermion compound, and the unusual electron transport has been attributed to the strong spin fluctuations and low carrier concentration (Kato *et al*., 2000).

In this study, we have measured magnetic circular dichroism (MCD) spectra at the transition-metal $L_{2,3}$ edges in the $D0_3$-type $(Fe_{1-x}V_x)_3Al$ in order to investigate their local magnetic moments and electronic structures. The magneto-optical sum rules for the core-level absorption (Carra *et al*., 1993, Stöhr & König, 1995, Thole *et al*., 1992) provide us a site-specific and independent determination of the spin and orbital contributions, μ_{spin} and μ_{orbit}, to the magnetic moment, which will also bring further insight into the electronic states involved.

2. Experimental

MCD measurements were performed at the beamline BL25SU of SPring-8, an 8 GeV electron storage ring of the Japan Synchrotron Radiation Research Institute. In this beamline, circularly polarized soft X-ray from a twin helical undulator was monochromatized with a spherical grating monochromator and focused on the sample position through pinholes of the permanent magnet circuit (Saitoh *et al*., 1998). Total photoelectroric yields, σ_+ and σ_-, were measured with an applied magnetic field B = 1.4 T along the direction parallel and anti-parallel to the soft X-ray photon spin, respectively. In the present study, the X-ray absorption (XAS) spectrum is defined as an average of these photoelectric yields, $(\sigma_+ + \sigma_-)/2$, and the MCD as a difference between them, $\sigma_+ - \sigma_-$. Photon energy $h\nu$ was calibrated by measuring a photoelectron spectrum of the Au $4f_{5/2}$ core level with its binding energy of 84.0 eV and the detector work function of 4.3 eV. The $D0_3$-type pseudo-binary $(Fe_{1-x}V_x)_3Al$ alloys were prepared in a size of 5 x 5 x 1 mm^3 for the MCD measurement. Details of the sample preparation are described elsewhere (Nishino *et al*., 1997). Clean surfaces were obtained for the photoelectric yield measurement by *in situ* scraping specimens with a diamond file. All the spectra were obtained at 20 K under a pressure of 3-5 x 10^{-8} Pa.

3. Results and Discussion

Typical MCD spectra at the Fe and V $L_{2,3}$ edges are shown in Figs.1 and 2 , respectively, with their XAS spectra for x = 0.3. In these figures, both the XAS and MCD spectra are normalized so that the spectral change at each L_3 edge is unity in the XAS spectrum. Structures around $h\nu$ = 530 eV in the V $L_{2,3}$ XAS spectrum are ascribed to the oxygen contamination on the optical components of the beamline and presumably also on the specimen surface, which could not be completely removed in the present measurement. However, the oxygen contamination seems not to affect the MCD spectrum, because no new MCD feature appears in around $h\nu$ = 530 eV. As seen in the figures, large MCD signals are observed at the Fe $L_{2,3}$ edges, while the V $L_{2,3}$ MCD spectrum has small but complicated structures. Although both the V $L_{2,3}$ MCD and XAS spectra reveal the importance of the interactions other than the spin-orbit one for this core-level absorption, the signs of the MCD readily indicate the antiferromagnetic coupling between the Fe and V moments. It is also noticed that the MCD signals, and hence the magnetic moments, for both V and Fe are reduced as the V composition x is increased.

The Fe-V antiferromagnetic coupling may be explained, at least for small x, as the V 3d polarization caused by the hybridizations of the V 3d states with the lower Fe 3d majority spin band and with the higher minority one. The resulting antibonding majority spin states, consisting mainly of the V 3d states, will be evacuated, while the V 3d dominant bonding minority spin states will be occupied. Thus the V moment will be aligned in antiparallel with the Fe moment. The observed antiferromagnetic coupling is in accordance with an Fe_8VAl_6 cluster calculation by the DV-$X\alpha$ method using the code SCAT (Adachi *et al*., 1978) and also with a recent theoretical work by

the charge- and spin-self-consistent Korringa-Kohn-Rostoker and coherent-potential approximation (KKR-CPA) method (Bansil *et al*., 1999).

According to the magneto-optical sum rules (Carra *et al*., 1993, Stöhr & König, 1995, Thole *et al*., 1992), μ_{spin} and μ_{orbit} can be derived from the integrated intensity of the $L_{2,3}$ MCD and XAS spectra as follows:

$$\mu_{orbit} = \frac{4}{3} n_H \frac{\int_{L_2+L_3} (\sigma_+ - \sigma_-) d\omega}{\int_{L_2+L_3} (\sigma_+ + \sigma_-) d\omega}, \quad (1)$$

and

$$\mu_{spin} = 2n_H \frac{\int_{L_3} (\sigma_+ - \sigma_-) d\omega - 2\int_{L_2} (\sigma_+ - \sigma_-) d\omega}{\int_{L_2+L_3} (\sigma_+ + \sigma_-) d\omega} + 7 < T_Z > . \quad (2)$$

Here, n_H is a number of the 3*d* holes and was assumed to be 4 for Fe and 7 for V, irrespective of *x*. The expectation value $<T_z>$ of the magnetic dipole moment may be averaged to zero for the polycrystalline sample and it was neglected. We also subtracted backgrounds arising from the transitions to the continuous states as the sum of two appropriate step-like functions and smoothed the V $L_{2,3}$ XAS spectrum in the O *K* edge region, as shown in Fig.2. Although it is difficult to apply the spin sum rule to the V $L_{2,3}$ edges because of the relatively small spin-orbit interaction, we tried to integrate the V $L_{2,3}$ MCD spectrum below and above the minimum of the XAS spectrum near $h\nu$ = 519 eV as the L_3 and L_2 regions, respectively, and roughly estimated the spin part of the V moment. In order to evaluate the errors associated with the integration interval for V, we tentatively divided the MCD spectrum into the L_2 and L_3 regions at $h\nu$ = 515 eV (the onset of the first dip) and 521 eV (the end of the second dip), and obtained 300 % and 15 % of the estimated value of μ_{spin}, respectively.

Orbital contributions thus estimated for both Fe and V are found to be almost quenched and less than 4 % of their spin parts. The total magnetic moment $\mu_{spin} + \mu_{orbit}$ on Fe decreases from 2.2 μ_B at x = 0 to 1.0 μ_B at x = 1/3, while that on V changes from –0.4 μ_B at x = 0.1 to –0.15 μ_B at x = 1/3. The total Fe moment for Fe_3Al agrees well with the average moment of 2.08 μ_B calculated by Bansil *et al*. (1999), but the V total moment is much smaller than the expected value of about –1.0 μ_B around x = 0.1. The obtained small value of the V moment may result from the present analysis without any correction for the sum rule; with the simple extrapolation of the correction factor in the reference of Teramura *et al*. (1996) to V^{2+}, the total magnetic moment on V would become about 3 times larger than the above estimated values.

The present analysis leads to the fairly large magnetization for Fe_2VAl, *i.e.* about one third of that for Fe_3Al, which seems inconsistent with the ordinary magnetization measurement (Kato *et al*., 2000). This is partially a result of the above-mentioned underestimation of the V moment and may be due to a magnetic cluster formed in the marginally magnetic Fe_2VAl compound. Large moments observed by the present MCD measurement might be associated with dynamical effects in the optical process involved or the marginal magnetic nature related to the spin fluctuations. Further experimental and theoretical studies are needed to clarify this point.

The synchrotron radiation experiments were performed at the SPring-8 with the approval of the Japanese Synchrotron Radiation Research Institute (JASRI) (Proposal No. 1997B1137-NS-np and 1999A0302-NS-np). We would like to appreciate the staff members of the SPring-8, especially Dr. T. Muro, Dr. M. Kotsugi, and Dr. R. Jung for their support during the course of the MCD measurement.

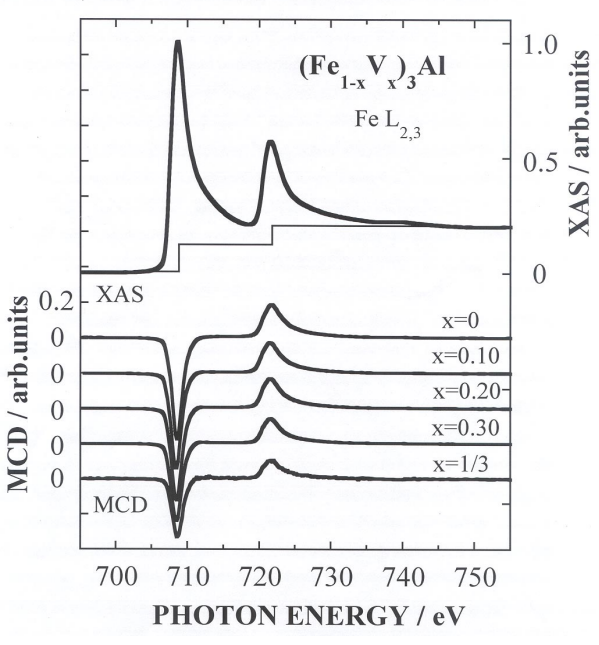

Figure 1.
Magnetic circular dichroism (MCD) spectra at the $L_{2,3}$ edges of Fe in the $D0_3$-type $(Fe_{1-x}V_x)_3Al$ with the various V composition *x*. An X-ray absorption spectrum (XAS) at the $L_{2,3}$ edges is also shown for x=0.3. Assumed two-step-like background is shown by thin lines.

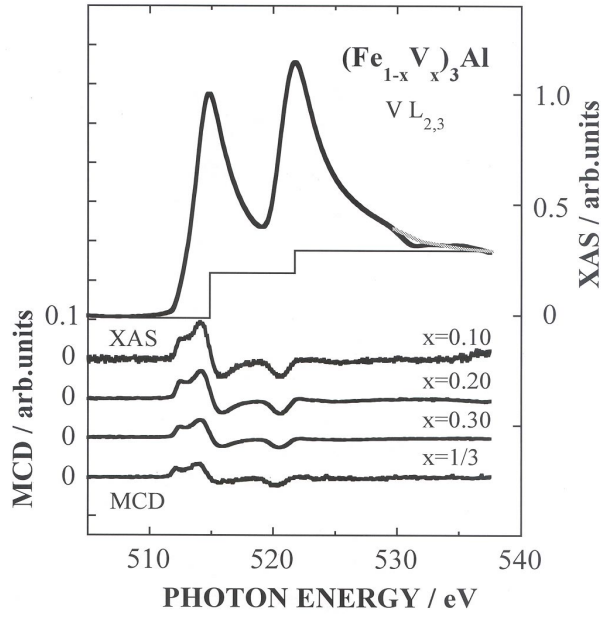

Figure 2.
Magnetic circular dichroism spectra (MCD) at the $L_{2,3}$ edges of V in the $D0_3$-type $(Fe_{1-x}V_x)_3Al$ with the various V composition *x*. An X-ray absorption (XAS) spectrum at the $L_{2,3}$ edges is also shown for x=0.3. Assumed two-step-like background and smoothed tail of the L_2 XAS spectrum are shown by thin lines and a gray curve, respectively.

Reference

Adachi, H., Tsukada, M. & Satoko, C. (1978) *J. Phys. Soc. Jpn*. **45**, 875-883.
Bansil, A., Kaprzyk, S., Mijnarends, P. E. & Tobola, J. (1999) *Phys. Rev. B.* **60**, 13396-13412.
Carra, P., Thole, B.T., Altarelli, M. & Wang, X. (1993) *Phys. Rev. Lett*. **70**, 694-697.
Kato, M., Nishino, Y., Mizutani, U. & Asano, S. (2000) *J. Phys.: Condens. Matter*. **12**, 1769-1779.
Nishino, Y., Kato, M., Asano, S., Soda, K., Hayasaki, M. & Mizutani, U. (1997) *Phys Rev Lett*. **79**, 1909-1912.
Saitoh, Y., Nakatani, T., Matsushita, T., Miyahara, T., Fujisawa, M., Soda, K., Muro, T., Ueda, S., Harada,• H., Sekiyama, A., Imada, S., Daimon, H. & Suga, S. (1998) *J. Synchrotron Rad*. **5**, 542-544.
Stöhr, J. & König, H. (1995) *Phys. Rev. Lett*. **75**, 3748-3751.
Teramura, Y., Tanaka, A., & Jo, T. (1996) *J. Phys. Soc. Jpn*. **65**, 1053-1055.
Thole, B.T., Carra, P., Sette, F., & van der Laan, G. (1992) *Phys. Rev. Lett.* **68**, 1943-1946.

 Received 31 July 2000 • Accepted 10 November 2000